Superharmonic Injection Locked Oscillators as Low Power Frequency Dividers

Hamid R. Rategh, Thomas H. Lee
Stanford University
Stanford, CA, USA

I. Abstract

Superharmonic injection locking is investigated in a new theoretical approach. Low power frequency dividers are designed using injection locked oscillators with cascode transistors. The Rockwell $0.5\mu m$ CMOS process is used to design a $3mW$ injection locked frequency divider in the $1800MHz$ frequency range. A $200MHz$ maximum locking range is achieved in simulations. 2SC3302 TOSHIBA NPN transistors are also used to build a $1.75mW$ injection locked frequency divider in the $800MHz$ frequency range to verify the theory.

II. Introduction

Forced oscillations in nonlinear oscillators were first analyzed by van der Pol [3] in a purely theoretical investigation. Adler [1] took an engineering approach and introduced the *locking range* figure of merit for an oscillator locked to the fundamental frequency of an incident signal. Others ([2],[4]) followed Adler's work and showed how an oscillator can be locked to a harmonic of an incident signal in what is conventionally called *subharmonic* locking.

In this work we show how an oscillator can be locked to an incident signal whose fundamental frequency equals a harmonic of the oscillator frequency in *superharmonic* locking, so that the oscillation frequency is an integer fraction of the fundamental frequency of the incident signal. We present a new method to calculate the locking range of an injection locked oscillator both for sub- and superharmonic locking. We also present a novel oscillator which is locked to half of the incident signal frequency.

III. Injection Locking

An LC oscillator can be modeled as a non-linear system $f(x)$, followed by a frequency selective system (e.g., RLC tank), $H(\omega)$, in a positive feedback loop. The nonlinear system includes all nonlinear elements plus any nonlinear amplitude limiting mechanism. The same model can be used for an injection locked oscillator with an external input (i.e., incident signal) as shown in fig. 1. To investigate the locking phenomenon in an injection locked oscillator, define the input, output, intermediate signal, and $H(\omega)$ as:

$$\nu_i(t) = V_i cos(\omega_i t + \phi) \tag{1}$$

$$\nu_o(t) = V_o cos(\omega_o t) \tag{2}$$

$$u(t) = f(e(t)) = f(\nu_o(t) + \nu_i(t)) \tag{3}$$

$$H(\omega) = \frac{H_0}{1 + j2Q\frac{\omega-\omega_r}{\omega_r}} \tag{4}$$

where, $\nu_i(t)$ is the incident signal, $\nu_o(t)$ is the output signal, ϕ is the phase difference between the two signals, ω_r and Q are the resonant frequency and quality factor of the RLC tank respectively. The output of the nonlinear element, $u(t)$, may have all the harmonics and intermodulation terms of $\nu_i(t)$ and $\nu_o(t)$, and can be written as:

$$u(t) = f(\nu_i + \nu_o) = \sum_{m=0}^{\infty}\sum_{n=0}^{\infty} K_{m,n} cos(m\omega_i t + m\phi) cos(n\omega_o t) \tag{5}$$

Each $K_{m,n}$ in (5) is an intermodulation coefficient defined as:

$$K_{m,0} = \frac{1}{2\pi}\int_{2\pi} L_m(V_o cos(\beta))d\beta \tag{6}$$

$$K_{m,n} = \frac{2}{2\pi}\int_{2\pi} L_m(V_o cos(\beta))cos(n\beta)d\beta \tag{7}$$

where

$$L_0(\nu_o) = \frac{1}{2\pi}\int_{2\pi} f(\nu_o + V_i cos(\alpha))d\alpha \tag{8}$$

$$L_m(\nu_o) = \frac{2}{2\pi}\int_{2\pi} f(\nu_o + V_i cos(\alpha))cos(m\alpha)d\alpha \tag{9}$$

We assume that all components of $u(t)$ far from the resonant frequency of the tank are filtered out and the output frequency can be written as: $\omega_o = \omega_r \pm \Delta\omega$. Thus, we only consider intermodulation terms with frequency of ω_o ($|m\omega_i - n\omega_o| = \omega_o$). For s-th order superharmonic injection locking (i.e., $\omega_o = \frac{1}{s}\omega_i$), the intermodulation terms with $n = sm \pm 1$ yield frequency equal to $\frac{1}{s}$ of the incident frequency. Likewise for subharmonic injection locking we have $m = (n \pm 1)s$. For a superharmonic injection locked oscillator, the signal $u_{\omega_o}(t)$, the component of $u(t)$ with frequency of ω_o, can be written as:

$$u_{\omega_o}(t) = K_{0,1} cos(\omega_o t) + \frac{1}{2}\sum_{m=1}^{\infty} K_{m,sm\pm1} cos(\omega_o t + m\phi) \tag{10}$$

Using a complex exponential to replace sines and cosines the output signal can be written as:

$$\nu_o = V_o e^{j\omega_o t} = \frac{H_0 e^{j\omega_o t}}{1 + j2Q\frac{\Delta\omega}{\omega_r}}[K_{0,1} + \frac{1}{2}\sum_{m=1}^{\infty} K_{m,sm\pm1} e^{jm\phi}] \tag{11}$$

0-7803-4766-8/$10.00 (c) 1998 IEEE

or,

$$V_o(1+j2Q\frac{\Delta\omega}{\omega_r}) = H_0[K_{0,1}+\frac{1}{2}\sum_{m=1}^{\infty}K_{m,sm\pm1}e^{jm\phi}] \quad (12)$$

The real and imaginary parts of (12) can be separated as:

$$V_o = H_o[K_{0,1}+\frac{1}{2}\sum_{m=1}^{\infty}K_{m,sm\pm1}cos(m\phi)] \quad (13)$$

$$2V_oQ\frac{\Delta\omega}{\omega_r} = \frac{H_0}{2}\sum_{m=1}^{\infty}K_{m,sm\pm1}sin(m\phi) \quad (14)$$

Equations (13) and (14) are the fundamental equations for a superharmonic injection locked oscillator. The simultaneous solution of these two equations yields V_o and ϕ. Equation (14) can be rearranged as:

$$\Delta\omega = (\frac{\omega_r}{2Q}\frac{V_i}{V_o})[\frac{H_0}{2V_i}\sum_{m=1}^{\infty}K_{m,sm\pm1}sin(m\phi)] \quad (15)$$

or,

$$\Delta\omega = \Delta\omega_A[\frac{H_0}{2V_i}\sum_{m=1}^{\infty}K_{m,sm\pm1}sin(m\phi)] \quad (16)$$

where $\Delta\omega_A$ is Adler's [1] *locking range* figure of merit. For the special case of $s=2$, (i.e., divide by two), and a third order nonlinearity (i.e., $f(x)=a_0+a_1x+a_2x^2+a_3x^3$), (13) and (14) can be solved analytically. The solution can be summarized as:

$$K_{1,1} = 2a_2V_oV_i$$

$$sin(\phi) = 4Q\frac{V_o}{H_0K_{1,1}}\frac{\Delta\omega}{\omega_r} = \frac{2Q}{H_oa_2V_i}\frac{\Delta\omega}{\omega_r}$$

$$\Rightarrow |\frac{\Delta\omega}{\omega_r}| < |\frac{H_0a_2V_i}{2Q}| \quad (17)$$

$$V_o = \sqrt{\frac{4}{3}\frac{1}{a_3H_0}[1-H_0(a_1+\frac{3}{2}a_3V_i^2+a_2V_icos(\phi))]} \quad (18)$$

As (17) suggests, the locking range $\frac{\Delta\omega}{\omega_r}$, can be increased by increasing the incident signal amplitude. The locking range can be increased until the term under the square root in (18) is non-negative. This means that the locking range can be increased as long as the oscillation condition, (i.e., loop gain of unity), can be satisfied.

It is important to remember that (13) and (14) are derived with the assumption that all the unwanted frequencies of $u(t)$ are filtered out by the RLC tank. So, one should design the oscillator to minimize any distortion caused by the incident signal to maximize the locking range.

One other observation is that the locking range depends on the amplitude of the incident signal. So, by injecting the incident signal to a high impedance node and resonating the injection node, one can reduce the required incident power significantly. As a result, MOS transistors are a good choice for injection locked oscillators with the incident signal injected to the gate of the MOS transistor.

IV. Simulations

A Colpitts oscillator is used as an injection locked frequency divider (divide by two). Fig. 2 shows the schematic of this divider. The incident signal is injected to the gate of transistor M1. A cascode is used for several reasons. First, the input and output are isolated, reducing output distortion by the incident signal. This helps to increase the locking range, as discussed previously. Secondly, the cascode has a higher output impedance than a single transistor, reducing the degradation of tank Q. Finally, M2 can be sized to be much smaller than M1, to reduce the junction capacitances at the output node. A bigger inductor can therefore be used for a given resonant frequency, increasing the effective parallel impedance of the RLC tank for a given tank Q. As a result a smaller current source can be used to bias the oscillator and still satisfy the oscillation condition. Using small sizes for M1 and M2 also reduces the current loss in the junction capacitors at the drain and source of M1 and M2 respectively.

The Rockwell $0.5\mu m$ CMOS process is used to design an injection locked divider for a DCS1800 radio system. The oscillator consumes $3mW$ of power and it is biased with a $2.5V$ supply and a $1.2mA$ current source. The inductors have a Q of 6 at the resonant frequency. An additional capacitor (Ctune) is added to switch from RX band to TX band.

A. Simulation results

The RX band divider has a free running oscillation at $920MHz$ with an amplitude of $181mV$ into a capacitive load. The TX band divider oscillates at $875MHz$ with $141mV$ of amplitude when there is no incident signal. The incident signal amplitude is swept between $50mV$ and $500mV$ $(-26dBV, -6dBV)$ and the locking range and output amplitude are measured.

Fig. 3 shows the output amplitude of the TX band divider as a function of the incident signal frequency. The output amplitude is almost symmetric around the center frequency ($f = 1750MHz$). As the incident signal amplitude increases, the maximum output amplitude also increases, until it reaches a maximum set by the effective parallel impedance of the RLC tank and the bias current. Here, this maximum occurs when Vi is around $200mV$. As the incident signal amplitude is raised beyond this level the output amplitude actually decreases. For the case of a third order nonlinear system, (18) also predicts the same output amplitude dependence on the incident signal amplitude. At large incident signal amplitudes the curves in fig. 3 are shifted to a slightly higher frequency range, because of the shift in the DC bias conditions due to the presence of a large incident signal. The DC voltage at the source of M1 increases as the incident signal amplitude increases. Consequently the source junction capacitance of M1 and also the junction capacitance of the biasing current source become smaller. As a result, the total capacitance at the source of M1, and consequently the total capacitance

seen at the output node, diminishes and the LC resonant frequency moves to a higher frequency.

The same simulation is repeated for the RX band divider and the results are shown in fig. 4. The same type of behavior is seen here too. However, the curve shift at large incident signals is greater than for the TX band divider, mainly because of the larger oscillation amplitudes in the RX band divider. This larger amplitude is due to the larger inductor Q at higher resonant frequencies, which leads to an effective larger parallel impedance of the tank.

Fig. 5 and 6 show the frequency range over which each divider can be injection locked or can function as a frequency divider for a given incident signal amplitude. As the incident signal amplitude increases, the locking range increases initially and then starts decreasing. The difference between high and low frequencies, the locking range, is plotted as a function of incident signal amplitude in fig. 7. For small incident signals the locking range is a linear function of the incident signal amplitude on a log scale. It is also important to note that the maximum achieved locking range for both TX and RX band divider is more than 2.5 times larger than the required range ($75MHz$ in each band). Thus can easily accommodate component tolerances and still tune the circuit over the required frequency range.

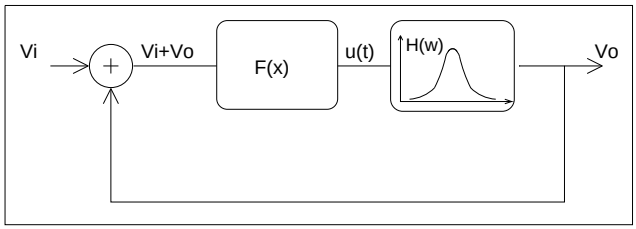

Fig. 1. Model for an injection locked oscillator

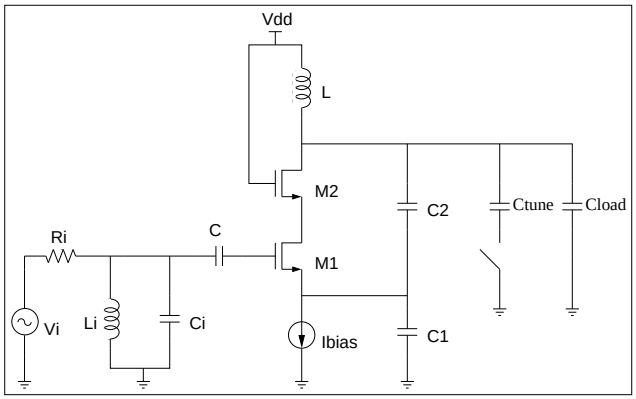

Fig. 2. Schematic of the injection locked frequency divider.

V. Experimental measurement

2SC3302 TOSHIBA NPN transistors are used to build a discrete injection locked frequency divider at $800MHz$. The same structure shown in fig. 2 with NPN transistors replacing the MOS transistors is used for the divider and striplines are used as inductors. The divider is biased with a $2.5V$ supply and the bias current is $0.7mA$. Fig. 8 shows the frequency range over which the oscillator can be used as a frequency divider for different incident signal amplitudes. The experimental measurements verify the theoretical and simulation predictions of the previous sections.

Fig. 9a shows the phase noise measurements for the free running oscillator, HP8648C signal generator (used as the incident signal), and the locked oscillator for different incident frequencies when in the amplitude of the incident signal is $-17dBV$. The difference between the input and output phase noise is shown in fig. 9b. For small offset frequencies the output has a $6dB$ better phase noise than the incident signal as expected. However, at higher offset frequencies where the injection locked divider does not follow the incident signal the noise of the divider increases the output phase noise. The output noise floor is also higher than the incident signal noise floor and it increases as the incident signal frequency approaches the edge of the locking range.

VI. Conclusion

A new method is reported to calculate the locking range for sub- and super-harmonic injection locked oscillators. A superharmonic injection locking technique is used to design low power frequency dividers in the $1800MHz$ frequency range. It is shown that cascode transistors can be used to design low power oscillators and also to enhance the locking range of injection locked frequency dividers. Using injection locking with cascode transistors, a maximum of $200MHz$ locking range (more than 10% of the center frequency) is achieved in a $3mW$ frequency divider at $1800MHz$. It is important to note that unlike conventional frequency dividers, the consumption power in an injection locked divider does not proportionally increase with frequency. At higher frequencies, higher Q inductors are available. So as long as the locking range does not limit us, it is possible to design oscillators with the same or even lower bias currents as for lower frequency oscillators. We believe that injection locked frequency dividers are a good alternative for digital CMOS frequency dividers, especially for low power and high frequency wireless systems.

VII. Acknowledgment

The authors would like to acknowledge Mr. Ali Hajimiri for his valuable discussions and comments.

VIII. References

[1] R. Adler, "A study of locking phenomena in oscillators," *Proceedings of the I.R.E and Waves and Electrons*, vol. 34, pp. 351–357, June 1946.

[2] A. S. Daryoush, T. Berceli, R. Saedi, P. R. Herczfeld, and A. Rosen, "Theory of subharmonic synchronization of nonlinear oscilators," *IEEE MTT-S Digest*, pp. 735–738, 1989.

[3] B. V. der Pol, "Forced oscillations in a circuit with nonlinear resistance," *Phil. Mag*, vol. 3, pp. 65–80, Jan. 1927.

[4] X. Zhang, X. Zhou, B. Aliener, and A. S. Daryoush, "A study of subharmonic injection locking for local oscillators," *IEEE Microwave and Guided Wave Letters*, vol. 2, pp. 97–99, Mar. 1992.

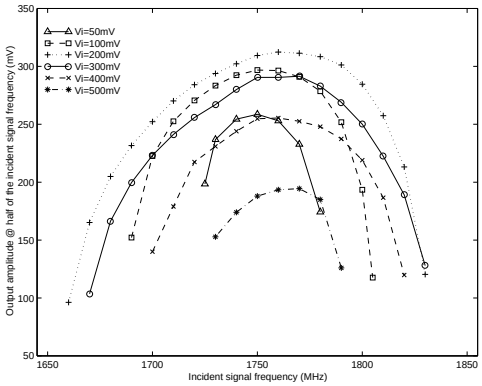

Fig. 3. Output amplitude for the TX band divider.

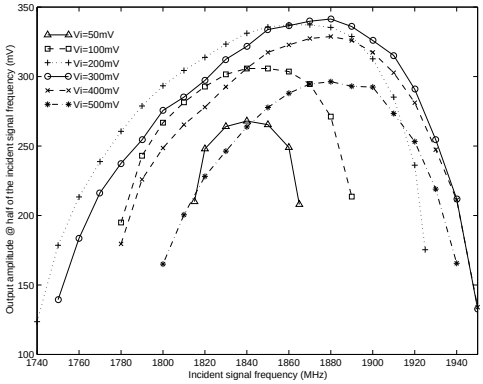

Fig. 4. Output amplitude for the RX band divider.

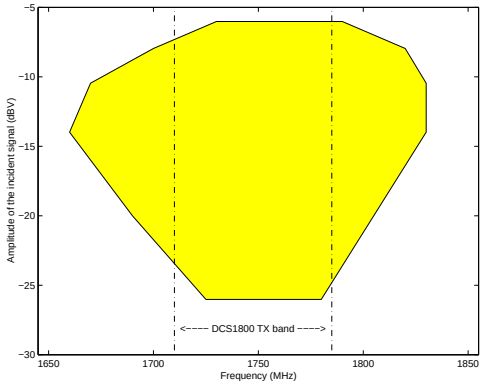

Fig. 5. Frequency range for the TX band divider.

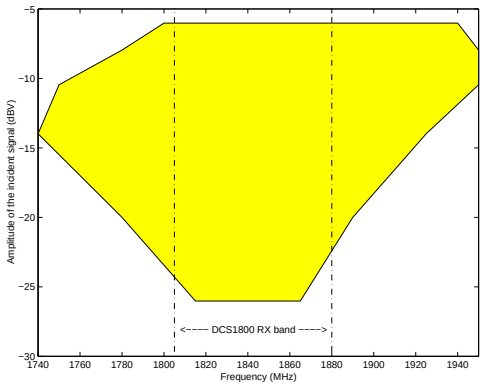

Fig. 6. Frequency range for the RX band divider.

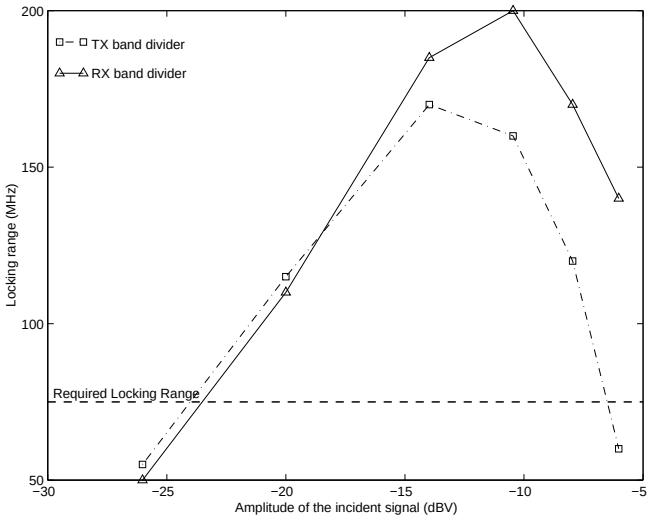

Fig. 7. Locking range for the TX and RX band dividers.

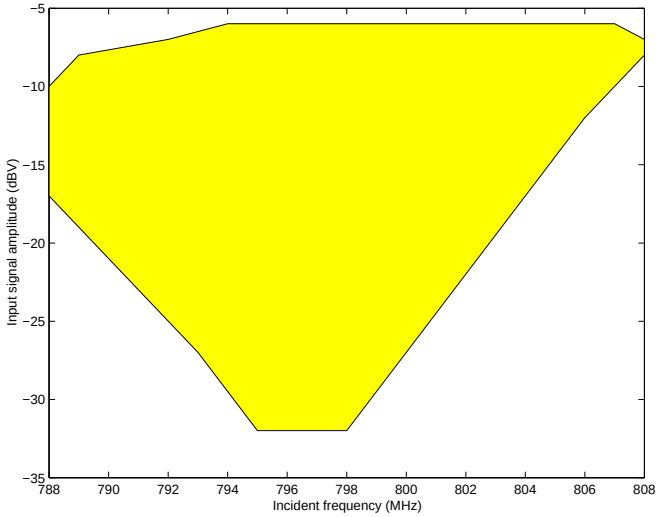

Fig. 8. Frequency range for the discrete circuit divider.

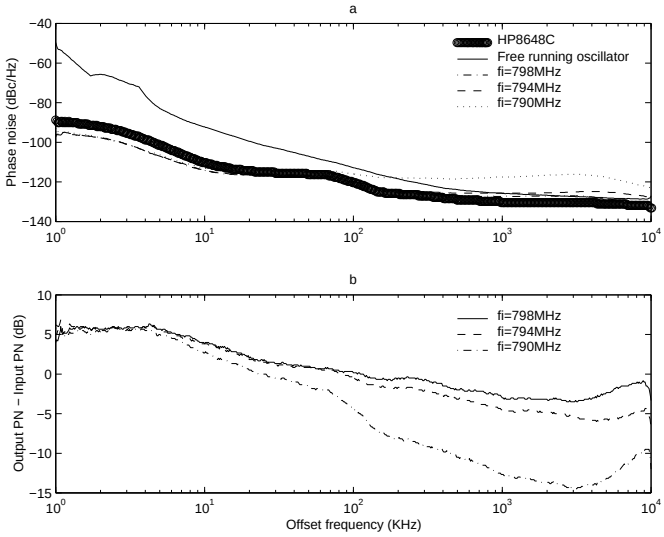

Fig. 9. Phase noise measurement of the discrete circuit divider.